Molecular Pharmacology Fast Forward. Published on May 18, 2006 as doi: 10.1124/mol.106.024711
This article has not been copyedited and formatted. The final version may differ from this version.

MOL #24711

Interaction studies of multiple binding sites on M_4 muscarinic acetylcholine receptors

Alfred A. Lanzafame[1], Patrick M. Sexton and Arthur Christopoulos

Drug Discovery Biology Laboratory, Department of Pharmacology, Monash University, Victoria 3800, Australia (A.C., P.M.S.) and Department of Pharmacology, University of Melbourne, Victoria 3010, Australia (A.L.).

Running Title: Allosteric cross-interactions at M_4 muscarinic receptors

***Address correspondence to:**

Assoc. Professor Arthur Christopoulos, B.Pharm., Ph.D.

Drug Discovery Biology Laboratory

Department of Pharmacology,

Building 13E, Monash University,

Clayton, 3800, Victoria, Australia

Phone: 61 3 9905 3817

Fax: 61 3 9905 5851

Email: arthur.christopoulos@med.monash.edu.au

Text pages	40
Tables	3
Figures	10
References	40
Abstract	244
Introduction	706
Discussion	1469

Non standard abbreviations:

C_7/3-phth, heptane-1,7-bis-(dimethyl-3'-phthalimidopropyl)-ammonium bromide, DMEM, Dulbecco's modified eagle's medium, dpm, disintegrations per minute, GPCR, G protein-coupled receptor, Gpp(NH)p, 5'-guanylyl-imidodiphosphate, KT5720, ((9S,10S,12R)-2,3,9,10,11,12-hexahydro-10-hydroxy-9-methyl-1-oxo-9,12-epoxy-1H-diindolo[1,2,3-fg:3_,2_,1_-kl]pyrrolo[3,4-i][1,6]benzodiazocine-10-carboxylic acid hexyl ester), mAChR, muscarinic acetylcholine receptor, McN-A-343, (4-(m-chlorophenylcarbamoyloxy)-2-butynyltrimethylammonium), TCM, ternary complex model, QCM, quaternary complex model, QNB, quinuclidinyl benzilate, WIN 51,708, 17-beta-hydroxy-17-alpha-ethynyl-5-alpha-androstano[3,2-b]pyrimido [1,2-a] benzimidazole, WIN 62,577, 17-beta-hydroxy- 17-alpha-ethynyl-delta(4)-androstano[3,2-b]pyrimido[1,2-a]benzimidazole.

Abstract

This study investigated the reciprocal cross-interactions between two distinct allosteric sites on the M_4 muscarinic acetylcholine receptor (mAChR) in the absence or presence of different orthosteric ligands. Initial studies revealed that two novel benzimidazole allosteric modulators, WIN 62,577 and WIN 51,708, exhibited different degrees of positive, negative or close to neutral cooperativity with the orthosteric site on M_1 or M_4 mAChRs, depending on the chemical nature of the orthosteric radioligand that was used ([^{3}H]N-methylscopolamine ([^{3}H]NMS) vs. [^{3}H]quinuclidinylbenzilate ([^{3}H]QNB)). The largest window for observing an effect (negative cooperativity) was noted for the combination of WIN 62,577 and [^{3}H]QNB at the M_4 mAChR. Experiments involving combination of these two ligands with unlabeled agonists (acetylcholine, McN-A-343 or xanomeline) revealed low degrees of negative cooperativity between WIN 62,577 and each agonist, whereas stronger negative cooperativity was observed against atropine. Interestingly, when these experiments were repeated using the prototypical modulators C_7/3-phth, alcuronium or brucine (which act at a separate allosteric site), WIN 62,577 exhibited negative cooperativity with each modulator when the orthosteric site was unoccupied, but this switched to neutral cooperativity when the receptor was occupied by [^{3}H]QNB. Dissociation kinetic experiments using [^{3}H]NMS and combination of C_7/3-phth with WIN 62,577 also provided evidence for neutral cooperativity between the two allosteric sites when the orthosteric site is occupied. Collectively, these results provide insight into the nature of the interaction between two distinct allosteric sites on the M_4 mAChR and how this interaction is perturbed upon occupancy of the orthosteric site.

Molecular Pharmacology Fast Forward. Published on May 18, 2006 as DOI: 10.1124/mol.106.024711
This article has not been copyedited and formatted. The final version may differ from this version.

Muscarinic acetylcholine receptors (mAChRs) are prototypical members of the Family A G protein-coupled receptor (GPCR) superfamily, and mediate the majority of the actions of acetylcholine (ACh) in both the periphery and the central nervous system. Although, these receptors are a focus of intense research as potential therapeutic targets, a significant challenge is the issue of high sequence conservation within the orthosteric domain across all five mAChR subtypes (Hulme et al., 1990; Wess, 1993). Such sequence conservation can account for the current paucity of orthosteric mAChR agonists and antagonists that display high selectivity for one mAChR subtype to the relative exclusion of all others. This problem is particularly pertinent to studies of the central nervous system, which is known to express all five subtypes of mAChR (Ehlert et al., 1995). Recent studies using mAChR knockout mice have highlighted the role of specific mAChRs in central disorders such as cognitive dysfunction, schizophrenia and a variety of pain states (Gomeza et al., 2001; Hamilton et al., 2001; Wess et al., 2003), and thus the ability to better target drugs to each of the mAChRs is of ongoing therapeutic relevance.

One potential avenue for achieving appropriate selectivity between mAChR subtypes is to target allosteric sites on these receptors, which are topographically distinct from the orthosteric site (Christopoulos et al., 1998). A number of studies have already revealed that there is at least one allosteric binding site common to structurally diverse small molecule mAChR modulators, such as gallamine (Clark and Mitchelson, 1976; Ellis and Seidenberg, 1989; 1992; Leppik et al., 1994), alcuronium (Jakubik et al., 1995; Proska and Tucek, 1994; Tucek et al., 1990; see Fig. 1) and heptane-1,7-bis-(dimethyl-3'-phthalimidopropyl)-ammonium bromide (C_7/3-phth) (Choo and Mitchelson, 1989; Christopoulos et al., 1993; Christopoulos and Mitchelson, 1994; Christopoulos et al., 1999; Lanzafame et al., 1997; see Fig. 1). Importantly, the effects of these prototypical mAChR allosteric ligands are all

consistent with a simple ternary complex model (TCM) of allosterism (Fig. 2A), which describes allosteric interactions in terms of ligand affinities for the free receptor and binding cooperativity between occupied orthosteric and allosteric sites (Ehlert, 1988; Lazareno and Birdsall, 1995; Christopoulos, 2002). The ability to describe mAChR allosteric interactions according to these mechanistic parameters means that useful quantitative measures can be derived for utilization in structure-activity studies of allosteric ligands.

Recently, Lazareno et al. (2002) reported that the benzimidazoles, 17-beta-hydroxy-17-alpha-ethynyl-5-alpha-androstano[3,2-b]pyrimido [1,2-a] benzimidazole (WIN 51,708), 17-beta-hydroxy- 17-alpha-ethynyl-delta(4)-androstano[3,2-b]pyrimido[1,2-a]benzimidazole (WIN 62,577) (see Fig. 1) and a series of related derivatives also act allosterically at mAChRs according to the TCM by exhibiting positive, negative or neutral co-operativity with [^{3}H]NMS and ACh depending on the mAChR subtype and orthosteric ligand bound to the receptor. However, it was revealed that these modulators do not appear to bind to the "common" allosteric site utilized by compounds such as gallamine, alcuronium and C_7/3-phth, but rather interact with a second allosteric site on mAChRs that also binds atypical modulators such as staurosporine and KT5720 ((9S,10S,12R)-2,3,9,10,11,12-hexahydro-10-hydroxy-9-methyl-1-oxo-9,12-epoxy-1H-diindolo[1,2,3-fg:3_,2_,1_-kl]pyrrolo[3,4-i][1,6]benzodiazocine-10-carboxylic acid hexyl ester) (Lazareno et al., 2000; 2002).

The presence of a second allosteric site on mAChRs raises a number of important questions. For example, it is currently unknown where the second allosteric site is located relative to the "common" allosteric site, as well as the orthosteric site. In addition, the nature and extent of possible interactions between the two allosteric sites and the orthosteric site are largely unexplored. This is particularly relevant for combination drug therapies, as allosteric

modulators have the potential to "engender" selectivity in otherwise non-selective ligands by virtue of their cooperative effects (Birdsall et al., 2001; Christopoulos, 2002; Christopoulos and Kenakin, 2002). Therefore, and given that the novel benzimidazole modulators are known to be centrally active (Lazareno et al., 2002), the present study investigated the interaction of these compounds with the M_1 and M_4 mAChRs, which represent the most abundant mAChR subtypes in the central nervous system and have been implicated as important targets for the pharmacotherapy of cognitive dysfunction associated with Alzheimer's disease (Whitehouse et al., 1982), schizophrenia and pain (Felder et al., 2000). In particular, the interaction between WIN 62,577 and a variety of orthosteric ligands and prototypical allosteric modulators was investigated in detail in order to gain additional insights into the nature of multi-site interactions on the M_4 mAChR.

Molecular Pharmacology Fast Forward. Published on May 18, 2006 as DOI: 10.1124/mol.106.024711
This article has not been copyedited and formatted. The final version may differ from this version.

Materials and Methods

Materials

Drugs and chemicals were obtained from the following sources: (-)-[^{3}H]-1-quinuclidinyl benzilate ([^{3}H]QNB) and [^{3}H]*N*-Methylscopolamine methyl chloride ([^{3}H]NMS) (NEN Life Science Products, Boston, MA, USA); Dulbecco's modified eagle's medium (DMEM), and geneticin (Life Technologies GIBCO BRL, Grand Island, NY, USA), fetal bovine serum (ThermoTrace, Melbourne, Victoria, Australia). C_7/3-phth was synthesized by the Institute for Drug Technology (Boronia, Victoria, Australia), alcuronium sulfate was a generous gift from Hoffmann-La Roche, Basel, Switzerland, and xanomeline tartrate was a generous gift from Eli Lilly, IN, USA. All other materials were obtained from Sigma Chemical Company (St. Louis, MO, USA).

Cell culture

Chinese hamster ovary (CHO-K1) cells, stably transfected with the human M_1 or M_4 mAChRs, were provided by Dr. M. Brann. Cells were grown and maintained in Dulbecco's modified Eagle's medium (DMEM) containing 20 mM HEPES, 10% fetal bovine serum, 50 μg/ml geneticin, for 4 days at 37°C in a humidified incubator containing 5% CO_2:95% O_2 before harvesting by trypsinization followed by centrifugation (300 g, 3 min) and resuspension of the pellet in DMEM.

Cell membrane preparations

CHO cells were grown, harvested and centrifuged as described above, with the final pellet resuspended in 5 ml of ice-cold Tris-HCl buffer (50 mM Tris, 3 mM $MgCl_2$ and 0.2 mM EGTA; pH 7.4 with HCl) and then homogenized using a Polytron homogenizer for three 10 s intervals at maximum setting with 30 s cooling periods employed between each burst. The

cell homogenate was centrifuged (1,000 g, 10 min, 25°C), the pellet discarded and the supernatant was re-centrifuged at 30,000 g for 30 min at 4°C. The resulting pellet containing cell membrane was resuspended in 5 ml of Tris-HCl buffer and protein content was determined using the method of Bradford (Bradford, 1976). The homogenate was then aliquoted into 1 ml amounts and stored frozen at -80°C until required for radioligand binding assays.

[^{3}H]NMS binding assays

Experiments were performed in HEPES buffer (110 mM NaCl, 5.4 mM KCl, 1.8 mM $CaCl_2$, 1 mM $MgSO_4$, 25 mM glucose, 50 mM HEPES, 58 mM sucrose; pH 7.4) using M_1 or M_4 CHO cell membrane homogenates (10 μg/assay tube in a total volume of 1 ml) incubated with [^{3}H]NMS (0.2 nM) and various concentrations of WIN 51,708 (1 nM to 0.1 mM), WIN 62,577 (1 nM to 0.1 mM) or ethanol vehicle equivalents for 1 hr at 37°C. The reaction was terminated by rapid filtration through Whatman GF/B filters using a Brandell cell harvester. Non-specific binding was determined using 10 μM atropine. Filters were washed three times with 4 ml aliquots of ice-cold saline and dried before radioactivity (dpm) was measured using liquid scintillation counting.

[^{3}H]QNB binding assays

Initial experiments were performed in HEPES buffer using M_1 or M_4 CHO cell membrane homogenates (10 μg/assay tube in a total volume of 1 ml) incubated with [^{3}H]QNB (0.05 or 0.1 nM) and various concentrations of WIN 51,708 (1 nM to 0.1 mM) or WIN 62,577 (1 nM to 0.1 mM) for 1 hr at 37°C. Subsequent experiments investigated the effects of the prototypical modulators, alcuronium (1 nM to 10 mM), brucine (10 nM to 10 mM) or C_7/3-phth (1 nM to 10 mM) on the binding of [^{3}H]QNB (0.1, 0.5 or 1 nM) in M_4 CHO membranes,

Molecular Pharmacology Fast Forward. Published on May 18, 2006 as DOI: 10.1124/mol.106.024711
This article has not been copyedited and formatted. The final version may differ from this version.

for 1 hr at 37°C. Combination binding experiments were also conducted using M_4 CHO membranes (20 μg/assay tube in a total volume of 1 ml) and investigating the effects of WIN 62,577 (10 nM to 0.1 mM) on the binding of [^{3}H]QNB (0.1 nM) in the absence or presence of the agonists, ACh (3 or 10 μM), 4-(m-chlorophenylcarbamoyloxy)-2-butynyltrimethylammonium) (McN-A-343; 3 or 10 μM), or xanomeline (0.1 or 0.3 μM), the orthosteric antagonist, atropine (3 or 6 nM), or the allosteric modulators, alcuronium (10, 30, 100, or 300 μM), brucine (10, 30, 100 or 300 μM) or C_7/3-phth (1, 3, 10, or 30 μM). To minimize the effect of G protein coupling on agonist binding, 5'-guanylyl-imidodiphosphate (Gpp(NH)p; 0.1 mM) was included in assay tubes for all agonist combination experiments. In all instances, incubation was for 1 hr at 37°C. All other details were as above.

[^{3}H]NMS dissociation kinetic assays

[^{3}H]NMS dissociation kinetic binding assays were performed in HEPES buffer, using a reverse time protocol. Initial experiments involved the determination of the complete time course of radioligand dissociation in the absence or presence of WIN 62 577. For these experiments, M_4 CHO membranes (10 μg/ assay tube in a total volume of 1 ml) were added to tubes containing [^{3}H]NMS (0.5 nM) in a time-staggered approach so that each replicate was allowed to equilibrate for 1 hr at 37°C. Once the receptors and radioligand had equilibrated, atropine (10 μM), in the absence or presence of WIN 62 577 (30 μM), was added at appropriate time intervals to prevent reassociation of [^{3}H]NMS to the M_4 mAChR. Non-specific binding was determined using atropine (10 μM). Subsequent dissociation experiments utilized a "two-point kinetic" approach (Kostenis and Mohr, 1996) to determine the radioligand dissociation rate constant in the presence of increasing concentrations of WIN 62,577 (1, 3, 10 or 30 μM) with or without the addition of C_7/3-phth (10 or 30 μM); [^{3}H]NMS binding was measured at the onset of dissociation (0 min) and at one other time point (10

Molecular Pharmacology Fast Forward. Published on May 18, 2006 as DOI: 10.1124/mol.106.024711
This article has not been copyedited and formatted. The final version may differ from this version.

min). This approach is valid if radioligand dissociation curves remain monophasic in the presence of modulator (see Data Analysis). All other details were as above.

Data analysis

Radioligand inhibition binding isotherms for all allosteric modulators when tested alone against either [^{3}H]NMS or [^{3}H]QNB were analyzed using Prism 4 (GraphPad Software, San Diego, CA) according to a simple equilibrium TCM (Fig. 2A) for allosteric interaction:

$$Y = \frac{[A]}{[A] + K_{App}} \qquad (1)$$

and

$$K_{App} = K_A \left(\frac{1 + [B]/K_B}{1 + \alpha \cdot [B]/K_B} \right) \qquad (2)$$

where Y denotes fractional receptor occupancy, [A] denotes the concentration and K_A the equilibrium dissociation constant, respectively, of the orthosteric radioligand, [B] denotes the concentration and K_B the equilibrium dissociation constant for the allosteric modulator, respectively, and α is the "cooperativity factor" for allosteric interaction between radioligand and modulator. This factor is a thermodynamic measure of the strength of allosteric interaction between two sites on the same GPCR, and is defined as the ratio of affinity of one ligand for the free receptor to its affinity for the receptor when the latter is occupied by the other ligand. Values of $\alpha > 1$ denote positive cooperativity (allosteric enhancement), values of $\alpha < 1$ denote negative cooperativity (allosteric inhibition), whereas values of $\alpha = 1$ denote neutral cooperativity.

Molecular Pharmacology Fast Forward. Published on May 18, 2006 as DOI: 10.1124/mol.106.024711
This article has not been copyedited and formatted. The final version may differ from this version.

Where necessary, a kinetic TCM was used instead for nonequilibrium binding data. For this latter analysis, the equations are as derived by Lazareno and Birdsall (1995), with the only modification being that the affinity constants in the original equations were re-cast as equilibrium dissociation constants (Avlani et al., 2004):

$$B_t = B_{AB} \cdot \left[1 - e^{-k_{onobs} \times t}\right] \qquad (3)$$

where

$$k_{onobs} = k_{offobs} \cdot \left(1 + \frac{[A]}{K_{App}}\right) \qquad (4)$$

$$k_{offobs} = \frac{k_{off} + \frac{[B] \cdot k_{offB}}{\left(K_B / \alpha\right)}}{1 + \frac{[B]}{\left(K_B / \alpha\right)}} \qquad (5)$$

and

$$B_{AB} = \frac{\frac{[A]}{K_{App}}}{1 + \frac{[A]}{K_{App}}} \qquad (6)$$

In these equations, B_{AB} denotes the fractional binding of the radioligand in the presence of modulator at equilibrium, k_{onobs} denotes the apparent association rate constant for the radioligand, k_{off} denotes the radioligand dissociation rate constant when the receptor is not occupied by modulator, k_{offB} denotes the radioligand dissociation rate constant for the modulator-occupied receptor, and all other parameters are as defined for equations 1 and 2. Equations 3-6 assume that the binding kinetics of each modulator are rapid relative to the

Molecular Pharmacology Fast Forward. Published on May 18, 2006 as DOI: 10.1124/mol.106.024711
This article has not been copyedited and formatted. The final version may differ from this version.

radioligand and that the modulator rapidly achieves equilibrium with the allosteric site, as is generally found for prototypical modulators of the mAChRs (Lazareno and Birdsall, 1995; Trankle et al., 2003).

Combination radioligand binding curves for WIN 62,577 *versus* [^{3}H]QNB in the absence and presence of various orthosteric ligands were analyzed according to the following equations (Christopoulos, 2000; Lazareno and Birdsall, 1995), based on an extended equilibrium TCM (Fig. 2B):

$$Y = \frac{100 \times ([A] + K_A)}{[A] + K_{App}} \qquad (7)$$

and

$$K_{App} = \frac{K_A K_B}{\alpha \cdot [B] + K_B} \cdot \left[1 + \frac{[I]^s}{K_I} + \frac{[B]}{K_B} + \frac{\alpha' \cdot [I]^s \cdot [B]}{K_I \cdot K_B} \right] \qquad (8)$$

where Y denotes percent specific binding, A, denotes the radioligand, B denotes the allosteric modulator, I denotes the orthosteric inhibitor, K_A, K_B and K_I denote their equilibrium dissociation constants, respectively, α denotes the cooperativity factor for the interaction between the allosteric modulator and the radioligand, α' denotes the cooperativity factor for the interaction between the modulator and the unlabeled orthosteric ligand, and s denotes an empirical slope factor. In all instances, this factor was not significantly different from unity and was constrained as such.

Molecular Pharmacology Fast Forward. Published on May 18, 2006 as DOI: 10.1124/mol.106.024711
This article has not been copyedited and formatted. The final version may differ from this version.

For the radioligand binding experiments involving the combination of WIN 62,577 with a prototypical allosteric modulator *versus* [^{3}H]QNB, a quaternary complex model (QCM) was used (Fig. 2C), which assumes that WIN 62,577 and either of the prototypical modulators bind to separate and distinct allosteric sites on the M_4 mAChR (Lazareno et al., 2002). Because of the profound effects of all modulators on radioligand kinetics, the data were obtained under pseudoequilibrium conditions and were thus analyzed according to a kinetic version of the QCM (Lazareno et al., 2002) using the following equations:

$$B_t = B_{ABC} \cdot \left[1 - e^{-k_{onobsBC} \times t}\right] \qquad (9)$$

$$k_{onobsBC} = k_{offobsBC} \cdot \left(1 + \frac{[A]}{K_{Mid}}\right) \qquad (10)$$

$$k_{offobsBC} = k_{off} \cdot \frac{\left[1 + \frac{[B] \cdot k_{off\,B}}{\left(K_B / \alpha\right)} + \frac{[C]\left(k_{off\,C} + \frac{k_{off\,BC} \cdot \delta[B]}{\left(K_B / \alpha\right)}\right)}{\left(K_C / \beta\right)}\right]}{\left[1 + \frac{[B]}{\left(K_B / \alpha\right)} + \frac{[C]\left(1 + \frac{\delta[B]}{\left(K_B / \alpha\right)}\right)}{\left(K_C / \beta\right)}\right]} \qquad (11)$$

Molecular Pharmacology Fast Forward. Published on May 18, 2006 as DOI: 10.1124/mol.106.024711
This article has not been copyedited and formatted. The final version may differ from this version.

$$K_{Mid} = K_A \left[\frac{1 + \left([B] / K_B \right) + \left([C] / K_C \right) \left[1 + \gamma \left([B] / K_B \right) \right]}{1 + \alpha \left([B] / K_B \right) + \beta \left([C] / K_C \right) \left[1 + \alpha\delta \left([B] / K_B \right) \right]} \right] \qquad (12)$$

$$B_{ABC} = \frac{B_{max} \cdot \frac{[A]}{K_{Mid}}}{1 + \frac{[A]}{K_{Mid}}} \qquad (13)$$

where B_{ABC} denotes the specific binding of the radioligand, A, in the presence of both modulators (B and C) at equilibrium, $k_{onobsBC}$ denotes the apparent association rate constant for the radioligand, k_{off} denotes the radioligand dissociation rate constant when the receptor is not occupied by any modulator, k_{offB} denotes the radioligand dissociation rate constant for the receptor when it is occupied by modulator, B, k_{offC} denotes the radioligand dissociation rate constant for the receptor when it is occupied by modulator, C, k_{offBC} denotes the radioligand dissociation rate constant for the receptor when it is occupied by both modulators, α represents the cooperativity factor for the interaction between ligands A and B, β represents the cooperativity factor for the interaction between ligands A and C, and γ and δ represent the cooperativity factors for interaction between ligands B and C when ligand A is either absent or present, respectively. K_A, K_B and K_C represent equilibrium dissociation constants for the binding of ligands A, B and C respectively. For this analysis, it was assumed that all modulators tested could completely prevent the dissociation of [^{3}H]QNB from the receptor, and thus the parameters k_{offB}, k_{offC} and k_{offBC} were constrained to a value of 0 min^{-1} in equation 11.

Molecular Pharmacology Fast Forward. Published on May 18, 2006 as DOI: 10.1124/mol.106.024711
This article has not been copyedited and formatted. The final version may differ from this version.

In all cases, potency, affinity and cooperativity factors were estimated as logarithms (Christopoulos, 1998). For curve-fitting, global nonlinear regression was performed whenever possible, whereby model parameters were constrained to be shared across multiple datasets. Comparisons between mean values were performed by unpaired *t* tests, as appropriate. Unless otherwise stated, values of $p < 0.05$ were taken as statistically significant.

Molecular Pharmacology Fast Forward. Published on May 18, 2006 as DOI: 10.1124/mol.106.024711
This article has not been copyedited and formatted. The final version may differ from this version.

Results

Binding properties of benzimidazole modulators at the M_1 and M_4 mAChR

Initial inhibition binding studies utilized the tropate, [^{3}H]NMS, as the orthosteric probe to characterize the interactions of each benzimidazole modulator at the M_1 or M_4 mAChRs. Both WIN 51,708 and WIN 62,577 inhibited the binding of [^{3}H]NMS at M_1 mAChRs in a concentration-dependent manner, but displayed an inability to fully abolish the specific binding of the radioligand (Figure 3A), indicative of low negative cooperativity (Table 1). An even weaker negative cooperative interaction was noted for WIN 62,577 against [^{3}H]NMS (Table 1), although the curve could not be fully determined due to the low affinity of the modulator for the receptor. Interestingly, when experiments were performed with WIN 51,708 at the M_4 mAChR, an enhancement of [^{3}H]NMS binding was observed with low concentrations of modulator, indicating positive cooperativity (Figure 3B). The subsequent inhibition seen with the highest concentrations of the modulator likely reflect a nonequilibrium state, as has been noted previously (Lazareno et al., 2002).

Because the magnitude and direction of cooperative interactions are dependent on the nature of the orthosteric probe, as well as the receptor subtype, subsequent experiments were undertaken using the benzilate, [^{3}H]QNB, as the radioligand. As with the [^{3}H]NMS experiments, both modulators inhibited [^{3}H]QNB binding at the M_1 mAChR, but with very weak negative cooperativity (Figure 4A; Table 1). Greater inhibition of [^{3}H]QNB binding was apparent at M_4 mAChRs; the interaction with WIN 62,577 exhibiting the highest degree of negative cooperativity noted in this study (Figure 4B; Table 1). In contrast to its positively cooperative interaction with [^{3}H]NMS, WIN 51,708 exhibited weak negative cooperativity with [^{3}H]QNB at the M_4 mAChR.

Molecular Pharmacology Fast Forward. Published on May 18, 2006 as DOI: 10.1124/mol.106.024711
This article has not been copyedited and formatted. The final version may differ from this version.

A comparison of the binding parameters for both modulators shown in Table 1 indicated that WIN 51,708 had a significantly higher affinity for the allosteric site on both M_4 and M_1 mAChRs than did WIN 62,577, with a preference for binding to the M_4 mAChR. Importantly, there was no significant difference between affinity estimates obtained at a particular subtype using either radioligand as probe ($p > 0.05$).

Interaction between WIN 62,577 and various orthosteric ligands at the M_4 mAChR

Although the interactions between either benzimidazole modulator and [^{3}H]NMS or [^{3}H]QNB were characterized by low levels of cooperativity, the combination of WIN 62,577 and [^{3}H]QNB nevertheless resulted in a sufficient effect range at the M_4 mAChR (approx. 50% maximal inhibition) such that additional experiments could be undertaken in the presence of unlabelled orthosteric ligands, which on their own would also be expected to further reduce levels of specific radioligand binding.

As shown in Figures 5 and 6, and summarized in Table 2, the interaction between WIN 62,577 and each orthosteric ligand was characterized by low degrees of negative cooperativity for the partial agonists McN-A-343 and xanomeline, and the antagonist, atropine, whereas slightly stronger negative cooperativity was noted for combination with the full agonist, ACh.

Interaction between WIN 62,577 and prototypical allosteric modulators at the M_4 mAChR

The interaction between WIN 62,577 and [^{3}H]QNB at the M_4 mAChR was also monitored in the absence and presence of various prototypical allosteric modulators. Because of the large number of parameters required to quantify these combination experiments according to the QCM (Fig. 2C), initial experiments investigated the interaction between each of the prototypical modulators alone against various concentrations of [^{3}H]QNB in order to obtain

Molecular Pharmacology Fast Forward. Published on May 18, 2006 as DOI: 10.1124/mol.106.024711
This article has not been copyedited and formatted. The final version may differ from this version.

measures of K_C and β that could then be utilized in the QCM fit of the combination data. Interestingly, both the C_7/3-phth (Fig. 7A) and, in particular, alcuronium (Fig. 8A) binding data were characterized by biphasic inhibition binding curves. Since multiphasic binding is not predicted by the simple equilibrium TCM, this finding suggested that the highest concentrations of each modulator were affecting the kinetics of [^{3}H]QNB binding to the M_4 mAChR to such an extent that equilibrium was not achieved. As a consequence, the data were fitted to a kinetic TCM (equations 3 - 6), rather than an equilibrium TCM, in order to derive the estimates of $LogK_C$ and Logβ shown in Table 3. In these equations, it was assumed that the modulators could completely prevent the dissociation of [^{3}H]QNB from the receptors, as has been shown previously for their effects on [^{3}H]NMS (Christopoulos et al., 1999; Lazareno et al., 1998; Trankle et al., 1997). Although the interaction between brucine and [^{3}H]QNB was also inhibitory, the curves were monophasic and resulted in complete inhibition of specific radioligand binding for all concentrations of [^{3}H]QNB tested (Fig. 9A). This finding suggests that the interaction between brucine and [^{3}H]QNB is either competitive or highly negatively cooperative. Analysis of the brucine/[^{3}H]QNB data according to either the equilibrium TCM (equations 1-2) or the kinetic TCM (equations 3 - 6) yielded essentially identical parameters (not shown), and thus the values from the (simpler) equilibrium TCM are reported in Table 3, where it can be seen that the nonlinear regression algorithm yielded a value of β that was indistinguishable from a value close to 0.

Subsequent combination experiments with WIN 62,577 and each of the prototypical modulators against [^{3}H]QNB yielded the curves shown in Figs. 7B - 9B. Because these experiments utilized a higher concentration of WIN 62,577 than the assays described in the preceding section, kinetic effects of WIN 62,577 on the equilibrium binding of the radioligand became evident; in each instance, the highest concentration of WIN 62,577

Molecular Pharmacology Fast Forward. Published on May 18, 2006 as DOI: 10.1124/mol.106.024711
This article has not been copyedited and formatted. The final version may differ from this version.

resulted in a profound drop in specific binding and yielded biphasic inhibition curves. The data were therefore globally fitted to a kinetic version of the QCM (equations 9 - 13) in order to derive modulator cooperativity factors for interaction on the [^{3}H]QNB-free receptor (γ) and the [^{3}H]QNB-occupied receptor (δ). The results of this analysis are shown in Table 3, where it can be seen that the interaction between modulators on the free receptor was characterized by different degrees of negative cooperativity; constraining the value of γ to either 0 (competitive interaction) or 1 (neutral cooperativity) did not provide a statistically better fit ($p > 0.05$; F-test). In contrast, the interaction between modulators on the radioligand-occupied receptor was found to be not significantly different from neutral cooperativity (δ=1), and this value was constrained as such when estimating the final parameter values shown in Table 3.

[^{3}H]NMS dissociation kinetic binding studies at the M_4 mAChR

Computer-assisted analysis of the interaction experiments described in the preceding section suggested that occupancy of the orthosteric site can change the interaction between two modulators occupying distinct allosteric sites on the M_4 mAChR from negatively cooperative to neutrally cooperative. Another experimental approach that can be used to independently verify this finding is to directly quantify the effects of one modulator on orthosteric radioligand dissociation kinetics in the absence or presence of the second modulator; by their very nature, dissociation kinetic experiments quantify interactions on a radioligand-occupied receptor, and thus provide direct information on the value of δ in the QCM. Unfortunately, the modest-to-high negative cooperativity between [^{3}H]QNB and each of the modulators tested at the M_4 mAChR made it practically difficult to establish dissociation kinetic concentration-effect curves for any modulator on the [^{3}H]QNB-occupied receptor, and so [^{3}H]NMS was used instead.

Molecular Pharmacology Fast Forward. Published on May 18, 2006 as DOI: 10.1124/mol.106.024711
This article has not been copyedited and formatted. The final version may differ from this version.

As shown in Fig 10A, 30μM WIN 62,577 was able to retard the observed dissociation rate constant of [^{3}H]NMS at the M_4 mAChR from 0.188 ± 0.006 min^{-1} to 0.106 ± 0.005 min^{-1} (n=5). Because the dissociation of radioligand in the absence and presence of modulator remained monophasic, subsequent experiments utilizing a range of WIN 62,577 concentrations employed a "two-point" kinetic experimental design (see Materials and Methods). Fig 10B shows the results of these experiments, where it can be seen that WIN 62,577 was able to concentration-dependently retard the dissociation of [^{3}H]NMS to 30 ± 3% (n=4) of the control radioligand k_{off} value determined in the absence of modulator. The Hill slope of the curve was not significantly different from unity ($p > 0.05$; F-test) and was constrained as such. According to the TCM, the $LogEC_{50}$ of the concentration-effect curve determined under these conditions represents the value of $Log(K_B/\alpha)$ for the modulator, which was determined to be -5.53 ± 0.10 (n=4).

Importantly, when these experiments were repeated in the presence of increasing concentrations of C_7/3-phth, the only effect noted was a reduction in the response range of WIN 62,577, with no significant alteration in the concentration-effect curve location parameter ($p > 0.05$; F-test). The reduction in the WIN 62,577 response window in the presence of C_7/3-phth is consistent with the ability of C_7/3-phth to reduce [^{3}H]NMS dissociation kinetics via an allosteric action in its own right; the lack of effect of C_7/3-phth on WIN 62,577 potency, however, can only be accommodated by assuming a lack of interaction between the two modulators, i.e. $\delta = 1$ on the [^{3}H]NMS-occupied receptor.

Molecular Pharmacology Fast Forward. Published on May 18, 2006 as DOI: 10.1124/mol.106.024711
This article has not been copyedited and formatted. The final version may differ from this version.

Discussion

This study has identified negative cooperativity between WIN 62,577 and prototypical modulators such as C_7/3-phth, alcuronium or gallamine, indicating distinct cross-interactions between two separate allosteric sites on the orthosteric ligand-free M_4 mAChR. Interestingly, the interactions exhibit neutral cooperativity when the orthosteric site on the M_4 mAChR is occupied by either [^{3}H]QNB or [^{3}H]NMS. These findings have important implications for combination drug therapies targeting disorders such as schizophrenia and pain, which are suggested to involve a significant M_4 mAChR component (Felder et al., 2000).

WIN 51,708 and WIN 62,577 were originally identified by Lazareno et al. (2002), and shown to exhibit different types of cooperativity with [^{3}H]NMS or ACh, depending on the mAChR involved. We have extended these observations to characterize the interaction between either modulator and [^{3}H]QNB. Our results highlight the dependence of allosteric interactions on the nature of the orthosteric ligand used as a "probe" to visualize the interaction. As shown previously for prototypical modulators (Hejnova et al., 1995; Lee and el-Fakahany, 1988), the tropate, [^{3}H]NMS, can exhibit quite different behaviors to the benzilate, [^{3}H]QNB, when tested against the same allosteric compound. In our study, [^{3}H]QNB exhibited negative cooperativity with either benzimidazole at M_1 and M_4 mAChRs, whereas WIN 51,708 was negatively cooperative with [^{3}H]NMS at the M_1 mAChR and positively cooperative at the M_4 mAChR; the apparent inhibition of [^{3}H]NMS binding by high concentrations of WIN 51,708 at the M_4 mAChR is likely due to a kinetic artifact related to the ability of the compound to slow [^{3}H]NMS equilibration time (Lazareno et al., 2002). Importantly, the TCM also predicts that the affinity of the modulator for the free receptor should be independent of the probe used to quantify the interaction (Ehlert, 1988). As shown in Table 1, this was indeed the case since

no significant differences were found between the $LogK_B$ estimates of either modulator determined using [^{3}H]NMS relative to [^{3}H]QNB.

The ligand-dependence of allosterism represents an important issue in drug discovery because orthosteric radioligands are still commonly used as receptor probes (Christopoulos, 2002). If the cooperativity between orthosteric and allosteric ligands is low, then standard binding assays will lack the power to differentiate weak allosteric modulation from a lack of effect. Our study provides a good example of the situation, where the combination of WIN 62,577 and [^{3}H]QNB at the M_4 mAChR yielded the best "window" of effect compared to all other combinations. For this reason, the combination of WIN 62,577 and [^{3}H]QNB was used to investigate the interactive properties of the modulator and other, unlabeled, orthosteric ligands. As shown in figures 5-6, and summarized in Table 2, the interaction between WIN 62,577 and any of the orthosteric agents was negatively cooperative at the M_4 mAChR. Interestingly, however, the degree of interaction was modest between WIN 62,577 and ACh but very weak between WIN 62,577 and the antagonist, atropine, or the agonists McN-A-343 and xanomeline. This suggests that it may be possible to attain a degree of absolute subtype selectivity, based on cooperativity rather than affinity, by manipulating the structure of WIN 62,577.

In addition to the original identification of WIN 51,708 and WIN 62,577 as novel, centrally-acting, mAChR modulators, another important finding by Lazareno et al. (2002) was that these compounds bound to a second allosteric site distinct from that recognized by prototypical modulators. Evidence supporting the notion of multiple allosteric sites on mAChRs was originally proposed in studies of tacrine (Potter and Ferrendelli, 1989) and Duo3 (Trankle and Mohr, 1997) on M_1 and M_2 mAChRs, but it was not until more recently

that studies of staurosporine and related compounds demonstrated a clear potential for reciprocal cross-reactions between more than one allosteric site on M_1 – M_4 mAChRs (Lazareno et al., 2000). These findings raise the exciting possibility that additional receptor binding domains exist that can provide greater receptor subtype-selectivity, but also, that the potential exists for combination therapies utilizing allosteric ligands.

A major component of our study focused on quantifying the interaction between WIN 62,577 and either C_7/3-phth, alcuronium and brucine. This required the extension of the TCM to a QCM, and the increased number of parameters meant that greater degrees of freedom were required to allow for a reliable fit of the model to the data. Initial experiments, therefore, were designed to obtain individual cooperativity factors for each modulator against [^{3}H]QNB. Interestingly, the studies involving C_7/3-phth or alcuronium were best fitted using a kinetic TCM, as these compounds yielded biphasic inhibition curves that were not in accord with the simple equilibrium TCM but were consistent with the ability of these compounds to slow radioligand kinetics. In addition, the interaction between brucine and [^{3}H]QNB was indistinguishable from simple competition, and indicates either high negative cooperativity or truly mutually exclusive binding.

For the allosteric modulator combination experiments, a kinetic version of the QCM was again required because of the profound effects of the highest concentrations of WIN 62,577 on [^{3}H]QNB kinetics, which explains the biphasic binding curves in figures 7B – 9B. From this analysis, we found that the curve fit was best resolved if the parameter, γ, was significantly different from either 1 or 0. This implies that the interaction between WIN 62,577 and either of the prototypical modulators was significantly different from neutral or mutually exclusive, respectively. For combination with C_7/3-phth, the interaction on the free

Molecular Pharmacology Fast Forward. Published on May 18, 2006 as DOI: 10.1124/mol.106.024711
This article has not been copyedited and formatted. The final version may differ from this version.

receptor was characterized by reasonably strong negative cooperativity, whereas for alcuronium or brucine the negative cooperativity was weak. Thus, the two allosteric sites on the M_4 mAChR have a definite potential for interaction. Furthermore, occupancy of the orthosteric site by [^{3}H]QNB resulted in the cooperativity between WIN 62,577 and either of the prototypical modulators becoming neutral ($\delta = 1$), suggesting that on the orthosteric site-occupied receptor, the interaction between the two allosteric sites can be dramatically modified. If neutral cooperativity between allosteric sites can be retained in the presence of other orthosteric ligands, it is possible that different modulators may be combined to produce additive effects with respect to modulation of the orthosteric site while having no effect on each other.

The additional use of dissociation kinetic experiments in our study was important because it allowed for an independent measurement of the parameter, δ, for the interaction between WIN 62,577 and C_7/3-phth on the [^{3}H]NMS-occupied receptor. Figure 10 shows that both C_7/3-phth and WIN 62,577 were able to cause a concentration-dependent retardation of [^{3}H]NMS dissociation from the M_4 mAChR. Because the potency of WIN 62,577 was unaltered by the presence of C_7/3-phth, this clearly indicated that the two modulators were not competing for the same site, but binding to separate sites with neutral cooperativity ($\delta = 1$). It should be noted that these dissociation kinetic experiments utilized [^{3}H]NMS instead of [^{3}H]QNB. Although use of the latter radioligand would have been preferred to allow for direct comparison with the pseudoequilibrium binding data, this was not possible due to the very slow dissociation time of [^{3}H]QNB under our assay conditions (not shown). Nevertheless, the direct demonstration of neutral cooperativity between two modulators on an orthosteric ligand-occupied receptor is sufficient to validate the concept.

Molecular Pharmacology Fast Forward. Published on May 18, 2006 as DOI: 10.1124/mol.106.024711
This article has not been copyedited and formatted. The final version may differ from this version.

It should also be noted that the experiments reported herein were conducted in a buffer containing high salt and high calcium concentrations. This buffer was chosen because we have previously used it for intact cell studies (Avlani et al., 2004; Lanzafame and Christopoulos, 2004) and wanted to ensure that ligand potencies were determined under similar assay conditions. However, the high ionic strength of this buffer, although appropriate for the extracellular milieu, is not physiological with respect to the intracellular milieu that is accessible in our membrane preparations. Nonetheless, we do not believe that this compromises our findings for the following reasons. First, the fact that high ionic strength reduces receptor-G protein interaction was actually a desired outcome, because we wanted to focus on interactions occurring on the free (uncoupled) receptor (hence our additional inclusion of Gpp(NH)p in all experiments involving agonists). Second, our estimates of the affinity and cooperativity of WIN 62,577 with [^{3}H]NMS and ACh are in excellent agreement with those obtained previously by Lazareno et al. (2000) using a different buffer to ours. Thus, we are confident that our findings are applicable to the intact cell situation, where the G protein-uncoupled state of the receptor is the predominant state (Kenakin, 1997), and the interactions we are quantifying are expected to occur at the extracellular face of the receptor.

In conclusion, this study has characterized the interaction of novel allosteric modulators of the M_1 and M_4 mAChR with a variety of orthosteric and prototypical allosteric modulators. In addition to confirming the presence of a second allosteric site on the M_4 mAChR, this study has derived quantitative estimates of cooperativity across three different binding sites on the M_4 mAChR, suggesting a greater window for discovery of subtype-selective allosteric modulators and/or development of combination drug therapies than previously anticipated.

References

Avlani VA, May LT, Sexton PM and Christopoulos A (2004) Application of a kinetic model to the apparently complex behaviors of negative and positive allosteric modulators of muscarinic acetylcholine receptors. *J Pharmacol Exp Ther* **308**:1062-1072.

Birdsall NJ, Lazareno S, Popham A and Saldanha J (2001) Multiple allosteric sites on muscarinic receptors. *Life Sci* **68**:2517-2524.

Choo LK and Mitchelson F (1989) Characterization of the antimuscarinic effect of heptane-1,7-bis-(dimethyl-3'-phthalimidopropyl ammonium bromide). *Eur J Pharmacol* **162**:429-435.

Christopoulos A (1998) Assessing the distribution of parameters in models of ligand-receptor interaction: to log or not to log. *Trends Pharmacol Sci* **19**:351-357.

Christopoulos A (2000) Quantification of allosteric interactions at G protein-coupled receptors using radioligand binding assays, in *Current Protocols In Pharmacology* (Enna SJ ed), Wiley and Sons, New York.

Christopoulos A (2002) Allosteric binding sites on cell-surface receptors: novel targets for drug discovery. *Nat Rev Drug Discov* **1**:198-210.

Christopoulos A and Kenakin T (2002) G protein-coupled receptor allosterism and complexing. *Pharmacol Rev* **54**:323-374.

Christopoulos A, Loiacono R and Mitchelson F (1993) Binding of the muscarine receptor antagonist heptane-1,7-bis(dimethyl-3'-phthalimidopropyl)ammonium bromide at cholinoceptor sites. *Eur J Pharmacol* **246**:1-8.

Christopoulos A and Mitchelson F (1994) Assessment of the allosteric interactions of the bisquaternary heptane-1,7-bis(dimethyl-3'-phthalimidopropyl)ammonium bromide at M1 and M2 muscarine receptors. *Mol Pharmacol* **46**:105-114.

Christopoulos A, Sorman JL, Mitchelson F and El-Fakahany EE (1999) Characterization of the subtype selectivity of the allosteric modulator heptane-1,7-bis-(dimethyl-3'-phthalimidopropyl) ammonium bromide (C7/3-phth) at cloned muscarinic acetylcholine receptors. *Biochem Pharmacol* **57**:171-179.

Clark AL and Mitchelson F (1976) The inhibitory effect of gallamine on muscarinic receptors. *Br J Pharmacol* **58**:323-331.

Ehlert FJ (1988) Estimation of the affinities of allosteric ligands using radioligand binding and pharmacological null methods. *Mol Pharmacol* **33**:187-194.

Ehlert FJ, Roeske WR and Yamamura HI (1995) Molecular biology, pharmacology, and brain distribution of subtypes of the muscarinic receptor, in *Psychopharmacology: The Fourth Generation of Progress* (Bloom FE and Kupfer DJ eds) pp 111-124, Raven Press, New York.

Ellis J and Seidenberg M (1989) Gallamine exerts biphasic allosteric effects at muscarinic receptors. *Mol Pharmacol* **35**:173-176.

Ellis J and Seidenberg M (1992) Two allosteric modulators interact at a common site on cardiac muscarinic receptors. *Mol Pharmacol* **42**:638-641.

Felder CC, Bymaster FP, Ward J and DeLapp N (2000) Therapeutic opportunities for muscarinic receptors in the central nervous system. *J Med Chem* **43**:4333-4353.

Gomeza J, Zhang L, Kostenis E, Felder CC, Bymaster FP, Brodkin J, Shannon H, Xia B, Duttaroy A, Deng CX and Wess J (2001) Generation and pharmacological analysis of M2 and M4 muscarinic receptor knockout mice. *Life Sci* **68**:2457-2466.

Hamilton SE, Hardouin SN, Anagnostaras SG, Murphy GG, Richmond KN, Silva AJ, Feigl EO and Nathanson NM (2001) Alteration of cardiovascular and neuronal function in M1 knockout mice. *Life Sci* **68**:2489-2493.

Hejnova L, Tucek S and el-Fakahany EE (1995) Positive and negative allosteric interactions on muscarinic receptors. *Eur J Pharmacol* **291**:427-430.

Hulme EC, Birdsall NJ and Buckley NJ (1990) Muscarinic receptor subtypes. *Annu Rev Pharmacol Toxicol* **30**:633-673.

Jakubik J, Bacakova L, el-Fakahany EE and Tucek S (1995) Subtype selectivity of the positive allosteric action of alcuronium at cloned M1-M5 muscarinic acetylcholine receptors. *J Pharmacol Exp Ther* **274**:1077-1083.

Kenakin TP (1997) *Pharmacologic Analysis of Drug-Receptor Interaction.* Lippincott-Raven, Philadelphia, PA

Kostenis E and Mohr K (1996) Two-point kinetic experiments to quantify allosteric effects on radioligand dissociation. *Trends Pharmacol Sci* **17**:280-283.

Lanzafame A, Christopoulos A and Mitchelson F (1997) Three allosteric modulators act at a common site, distinct from that of competitive antagonists, at muscarinic acetylcholine M2 receptors. *J Pharmacol Exp Ther* **282**:278-285.

Lanzafame A and Christopoulos A (2004) Investigation of the interaction of a putative allosteric modulator, SCH-202676, with M_1 muscarinic acetylcholine receptors. *J Pharmacol Exp Ther* **308**:830-837

Lazareno S and Birdsall NJ (1995) Detection, quantitation, and verification of allosteric interactions of agents with labeled and unlabeled ligands at G protein-coupled receptors: interactions of strychnine and acetylcholine at muscarinic receptors. *Mol Pharmacol* **48**:362-378.

Lazareno S, Gharagozloo P, Kuonen D, Popham A and Birdsall NJ (1998) Subtype-selective positive cooperative interactions between brucine analogues and acetylcholine at muscarinic receptors: radioligand binding studies. *Mol Pharmacol* **53**:573-589.

Lazareno S, Popham A and Birdsall NJ (2000) Allosteric interactions of staurosporine and other indolocarbazoles with N-[methyl-(3)H]scopolamine and acetylcholine at muscarinic receptor subtypes: identification of a second allosteric site. *Mol Pharmacol* **58**:194-207.

Lazareno S, Popham A and Birdsall NJ (2002) Analogs of WIN 62,577 define a second allosteric site on muscarinic receptors. *Mol Pharmacol* **62**:1492-1505.

Lee NH and el-Fakahany EE (1988) Influence of ligand choice on the apparent binding profile of gallamine to cardiac muscarinic receptors. Identification of three main types of gallamine-muscarinic receptor interactions. *J Pharmacol Exp Ther* **246**:829-838.

Leppik RA, Miller RC, Eck M and Paquet JL (1994) Role of acidic amino acids in the allosteric modulation by gallamine of antagonist binding at the m2 muscarinic acetylcholine receptor. *Mol Pharmacol* **45**:983-990.

Potter LT and Ferrendelli CA (1989) Affinities of different cholinergic agonists for the high and low affinity states of hippocampal M1 muscarine receptors. *J Pharmacol Exp Ther* **248**:974-978.

Proska J and Tucek S (1994) Mechanisms of steric and cooperative actions of alcuronium on cardiac muscarinic acetylcholine receptors. *Mol Pharmacol* **45**:709-717.

Trankle C, Elis K, Wiese M and Mohr K (1997) Molecular rigidity and potency of bispyridinium type allosteric modulators at muscarinic M2-receptors. *Life Sci* **60**:1995-2003.

Trankle C and Mohr K (1997) Divergent modes of action among cationic allosteric modulators of muscarinic M2 receptors. *Mol Pharmacol* **51**:674-682.

Trankle C, Weyand O, Voigtlander U, Mynett A, Lazareno S, Birdsall NJ and Mohr K (2003) Interactions of orthosteric and allosteric ligands with [3H]dimethyl-W84 at the common allosteric site of muscarinic M2 receptors. *Mol Pharmacol* **64**:180-190.

Tucek S, Musilkova J, Nedoma J, Proska J, Shelkovnikov S and Vorlicek J (1990) Positive cooperativity in the binding of alcuronium and N-methylscopolamine to muscarinic acetylcholine receptors. *Mol Pharmacol* **38**:674-680.

Wess J (1993) Mutational analysis of muscarinic acetylcholine receptors: structural basis of ligand/receptor/G protein interactions. *Life Sci* **53**:1447-1463.

Wess J, Duttaroy A, Gomeza J, Zhang W, Yamada M, Felder CC, Bernardini N and Reeh PW (2003) Muscarinic receptor subtypes mediating central and peripheral antinociception studied with muscarinic receptor knockout mice: a review. *Life Sci* **72**:2047-2054.

Whitehouse PJ, Price DL, Struble RG, Clark AW, Coyle JT and Delon MR (1982) Alzheimer's disease and senile dementia: loss of neurons in the basal forebrain. *Science* **215**:1237-1239.

Footnotes

The authors would like to thank Ms. Elizabeth Guida for excellent technical assistance. This work was funded by project grant no. 400134 of the National Health and Medical Research Council (NHMRC) of Australia. AC and PMS are Senior Research Fellows of the NHMRC.

Address reprint requests to:

Assoc. Professor Arthur Christopoulos, B.Pharm., Ph.D.

Drug Discovery Biology Laboratory

Department of Pharmacology,

Building 13E, Monash University,

Clayton, 3800, Victoria, Australia

Phone: 61 3 9905 3817

Fax: 61 3 9905 5851

Email: arthur.christopoulos@med.monash.edu.au

[1] Present address: Metabolic Pharmaceuticals Ltd., Baker Heart Research Institute, Prahran, Vic, Australia, 3141

Molecular Pharmacology Fast Forward. Published on May 18, 2006 as DOI: 10.1124/mol.106.024711
This article has not been copyedited and formatted. The final version may differ from this version.

Figure Legends

Figure 1 Structures of allosteric modulators used in this study.

Figure 2 Allosteric models investigated in this study. **(A)** A simple ternary complex model (TCM) of allosteric interaction. **(B)** An extended TCM for the interaction of two orthosteric ligands and one allosteric modulator on the same receptor. **(C)** A quaternary complex model (QCM) for the interaction of two allosteric modulators (each binding to a different allosteric site) and one orthosteric ligand on the same receptor. In these models, **R** represents the receptor, **A** represents orthosteric radioligand, **B** and **C** represent allosteric modulators, **I** represents an unlabeled orthosteric ligand, $\mathbf{K_A}$, $\mathbf{K_B}$, $\mathbf{K_C}$ and $\mathbf{K_I}$ represent equilibrium dissociation constants for the binding of ligands A, B, C and I respectively, α represents the cooperativity factor for the allosteric interaction between ligands A and B, α' represents the cooperativity factor for the interaction between ligands B and I, β represents the cooperativity factor for the interaction between ligands A and C, and γ and δ represent the cooperativity factors for the interaction between ligands B and C when ligand A is absent or present, respectively. When $\gamma=\delta=\mathbf{0}$, the allosteric modulators bind to same site ("infinite" negative cooperativity), $\gamma=\delta=\mathbf{1}$ the allosteric modulators bind to separate sites and there is no interaction (neutral cooperativity).

Figure 3 Inhibition binding of the allosteric modulators, WIN 51,708 (●), WIN 62,577 (■), or ethanol vehicle (✳) against 0.2 nM [^{3}H]NMS at the M_1 mAChR **(A)** or M_4 mAChR **(B)** expressed in CHO cell membranes. Incubation was for 1 hr at 37°C in HEPES buffer, pH 7.4. Non-specific binding was defined by 10 μM atropine. Data points represent the mean ± SEM of 3 experiments conducted in duplicate.

Molecular Pharmacology Fast Forward. Published on May 18, 2006 as DOI: 10.1124/mol.106.024711
This article has not been copyedited and formatted. The final version may differ from this version.

Figure 4 Inhibition binding of the allosteric modulators, WIN 51,708 (●), WIN 62,577 (■), or ethanol vehicle (✳) against 0.1 nM [^{3}H]QNB at the M_1 mAChR **(A)** or M_4 mAChR **(B)** expressed in CHO cell membranes. Data points represent the mean ± SEM of 3 experiments conducted in duplicate. All other details as for Figure 3.

Figure 5 Inhibition binding of WIN 62,577 against 0.1 nM [^{3}H] QNB in the absence (■) and presence of 3 μM (▼), 10 μM (●) ACh **(A)**, or McN-A-343 **(B)**, at the M_4 mAChR expressed in CHO cell membranes. Experiments using agonists were conducted in the presence of Gpp(NH)p (100 μM). Data points represent the mean ± SEM of 3-5 experiments conducted in duplicate. All other details as for Figure 3.

Figure 6 Inhibition binding of WIN 62,577 against 0.1 nM [^{3}H] QNB in the absence (■) and presence of **(A)** 0.1 μM (▼) or 0.3 μM (●) xanomeline, or **(B)** 3 nM (◆) or 6 nM (▲) atropine, at the M_4 mAChR expressed in CHO cell membranes. Experiments using agonists were conducted in the presence of Gpp(NH)p (100 μM). Data points represent the mean ± SEM of 3-5 experiments conducted in duplicate. All other details as for Figure 3.

Figure 7 (A) Inhibition binding of C_7/3-phth against 0.1 nM (■), 0.5 nM (▲), or 1 nM (▼) [^{3}H] QNB. **(B)** Inhibition binding of WIN 62,577 against [^{3}H] QNB in the absence (■) and presence of 1 μM (▲), 3 μM (▼), 10 μM (◆) or 30 μM (●) C_7/3-phth. All experiments were performed using CHO cell membranes expressing the M_4 mAChR. Data points represent the mean ± SEM of 3-5 experiments conducted in duplicate. All other details as for Figure 3.

Figure 8 **(A)** Inhibition binding of alcuronium against 0.1 nM (■), 0.5 nM (▲), or 1 nM (▼) [^{3}H] QNB. **(B)** Inhibition binding of WIN 62,577 against [^{3}H] QNB in the absence (■) and presence of 10 μM (▲), 30 μM (▼), 100 μM (◆) or 300 μM (●) alcuronium. All experiments were performed using CHO cell membranes expressing the M_4 mAChR. Data points represent the mean ± SEM of 3-5 experiments conducted in duplicate. All other details as for Figure 3.

Figure 9 **(A)** Inhibition binding of brucine against 0.1 nM (■), 0.5 nM (▲), or 1 nM (▼) [^{3}H] QNB. **(B)** Inhibition binding of WIN 62,577 against [^{3}H] QNB in the absence (■) and presence of 10 μM (▲), 30 μM (▼), 100 μM (◆) or 300 μM (●) brucine. All experiments were performed using CHO cell membranes expressing the M_4 mAChR. Data points represent the mean ± SEM of 3-5 experiments conducted in duplicate. All other details as for Figure 3.

Figure 10 **(A)** Effect of WIN 62,577 on the dissociation rate of [^{3}H]NMS in CHO membranes expressing the M_4 mAChR. Membranes were incubated with 0.5 nM [^{3}H]NMS at 37°C for 1 hr in HEPES buffer, pH 7.4, before dissociation was revealed by addition of 1 μM atropine alone (■) or in combination with 30 μM WIN 62,577 (●) or ethanol vehicle (✳). **(B)** Concentration-dependent effects of WIN 62,577 on the [^{3}H]NMS-occupied receptor in the absence (■) and presence of 10 μM (●), 30 μM (▲), or 100 μM (▼) C_7/3-phth. The dissociation rate constant of [^{3}H]NMS from M_4 mAChRs was measured using a two-time point kinetic protocol and expressed as percentage of control. Data points represent the mean ± SEM of 3-5 experiments conducted in duplicate.

Molecular Pharmacology Fast Forward. Published on May 18, 2006 as DOI: 10.1124/mol.106.024711
This article has not been copyedited and formatted. The final version may differ from this version.

Tables

Table 1 Inhibition binding parameters for benzimidazole allosteric modulators using [^{3}H]NMS or [^{3}H]QNB at M_1 or M_4 mAChRs in CHO cell membranes. Parameters derived from nonlinear regression analysis are presented as the mean ± SEM (n=3-4).

Ligand	M_1 mAChR		M_4 mAChR	
	Log K_B[a]	Log α[b]	Log K_B[a]	Log α[b]
[^{3}H]NMS				
WIN 51,708	-6.01 ± 0.12	-0.23 ± 0.01[*†]	-6.34 ± 0.21[*]	0.68 ± 0.15[*†]
		(0.59)		(4.77)
WIN 62,577	-5.38 ± 0.35	-0.75 ± 0.05[*]	-5.41 ± 0.31[*]	-0.14 ± 0.04[*]
		(0.18)		(0.73)
[^{3}H]QNB				
WIN 51,708	-5.98 ± 0.04[*†]	-0.15 ± 0.01[*†]	-6.29 ± 0.26[*†]	-0.38± 0.01[*†]
		(0.71)		(0.42)
WIN 62,577	-5.35 ± 0.05[*†]	-0.39± 0.01[*†]	-5.60 ± 0.05[*†]	-0.60± 0.01[*†]
		(0.40)		(0.25)

[a] Logarithm of the modulator equilibrium dissociation constant.

[b] Logarithm of the cooperativity factor. Antilogarithm (geometric mean) shown in parentheses.

[*] Student's t test found a significant ($p < 0.05$) difference between WIN 51,708 and WIN 62,577 parameters.

[†] Student's t test found a significant ($p < 0.05$) difference between M_1 and M_4 mAChR groups.

Molecular Pharmacology Fast Forward. Published on May 18, 2006 as DOI: 10.1124/mol.106.024711
This article has not been copyedited and formatted. The final version may differ from this version.

Table 2 Inhibition binding parameters for WIN 62,577 against [^{3}H]QNB in combination with a range of orthosteric ligands at M_4 mAChRs in CHO cell membranes. Parameters derived from nonlinear regression analysis are presented as the mean ± SEM (n=5).

Ligand	Log K_A[a]	Log K_B[a]	Log K_I[a]	Log α[b]	Log β[c]
QNB	-10.2 ± 0.05	-	-	-0.60 ± 0.01 (0.25)	-
Atropine	-	-	-8.73 ± 0.04	-	-0.27 ± 0.01 (0.54)
ACh	-	-	-5.32 ± 0.02	-	-0.92 ± 0.01 (0.12)
McN-A-343	-	-	-5.29 ± 0.02	-	-0.30 ± 0.03 (0.50)
Xanomeline	-	-	-7.50 ± 0.04	-	-0.27 ± 0.01 (0.54)
WIN 62,577	-	-5.47 ± 0.04	-	-	-

[a] Logarithm of each ligand's equilibrium dissociation constant based on the extended TCM reaction scheme shown in Figure 2.

[b] Logarithm of the cooperativity factor for the interaction between WIN 62,577 and [^{3}H]QNB. Antilogarithm (geometric mean) shown in parentheses.

[c] Logarithm of the cooperativity factor for the interaction between WIN 62,577 and the indicated unlabeled orthosteric ligand. Antilogarithm (geometric mean) shown in parentheses.

Molecular Pharmacology Fast Forward. Published on May 18, 2006 as DOI: 10.1124/mol.106.024711
This article has not been copyedited and formatted. The final version may differ from this version.

Table 3 Radioligand binding parameters for the interaction between [^{3}H]QNB, WIN 62,577 and C_7/3-phth, alcuronium or brucine at the M_4 mAChR. Parameters derived from nonlinear regression analysis are presented as the mean ± SEM (n=3-5).

Allosteric modulator	Log K_B[a]	Log α[b]	Log β[c]	Log γ[d]	Log δ[e]
C_7/3-phth	-5.81 ± 0.22	-	-2.69 ± 0.03 (0.002)	-1.02 ± 0.04 (0.096)	0 (1)
Alcuronium	-4.50 ± 0.06	-	-1.49 ± 0.04 (0.032)	-0.60 ± 0.03 (0.25)	0 (1)
Brucine	-4.64 ± 0.03	-	-100 [f] (~ 0)	-0.31± 0.06 (0.49)	0 (1)
WIN 62,577	-5.32 ± 0.07	-0.79 ± 0.01 (0.16)	-	-	-

[a] Logarithm of the modulator equilibrium dissociation constant at the free receptor.

[b] Logarithm of the cooperativity factor for the interaction between WIN 62,577 and [^{3}H]QNB. Antilogarithm (geometric mean) shown in parentheses.

[c] Logarithm of the cooperativity factor for the interaction between the indicated prototypical modulator and [^{3}H]QNB. Antilogarithm (geometric mean) shown in parentheses.

[d] Logarithm of the cooperativity factor for the interaction between WIN 62,577 and the indicated prototypical modulator on the [^{3}H]QNB-free receptor. Antilogarithm (geometric mean) shown in parentheses.

[e] Logarithm of the cooperativity factor for the interaction between WIN 62,577 and the indicated prototypical modulator on the [^{3}H]QNB-occupied receptor. Antilogarithm (geometric mean) shown in parentheses. In all instances, the value for Log δ was determined

by an extra-sum-of squares test (F test) to not be significantly different from 0 (i.e., $\delta = 1$), and was constrained as such in the analyses.

[f] Irrespective of initial values, the nonlinear regression algorithm always converged to the arbitrarily assigned boundary value of Log $\beta = -100$, indicating that the degree of negative cooperativity between brucine and [^{3}H]QNB was so high that it could not be distinguished from competition ($\beta = 0$).

Molecular Pharmacology Fast Forward. Published on May 18, 2006 as DOI: 10.1124/mol.106.024711
This article has not been copyedited and formatted. The final version may differ from this version.

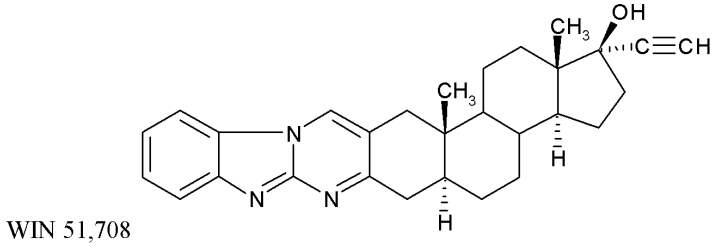

WIN 51,708

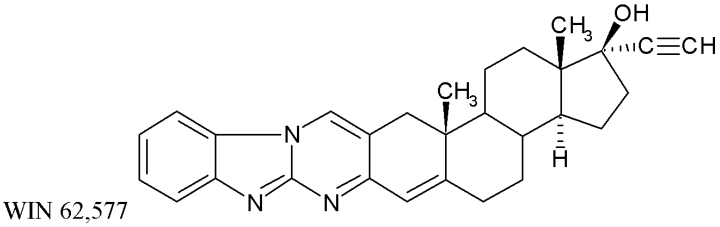

WIN 62,577

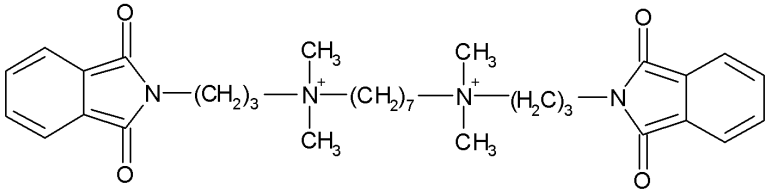

C_7/3-phth

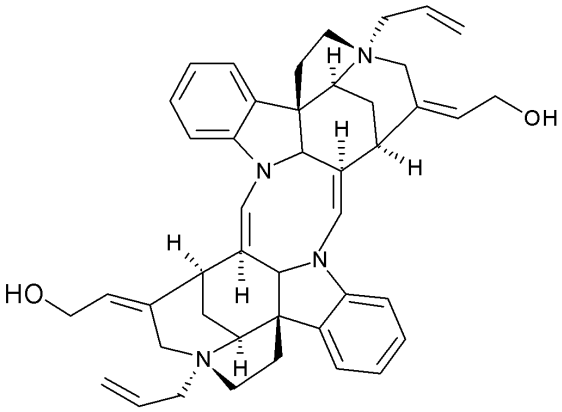

Alcuronium

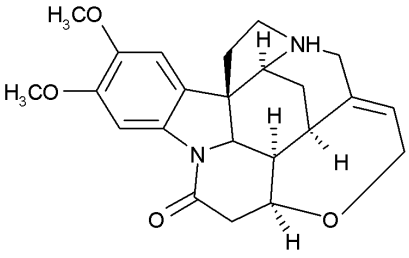

Brucine

Figure 1

Molecular Pharmacology Fast Forward. Published on May 18, 2006 as DOI: 10.1124/mol.106.024711
This article has not been copyedited and formatted. The final version may differ from this version.

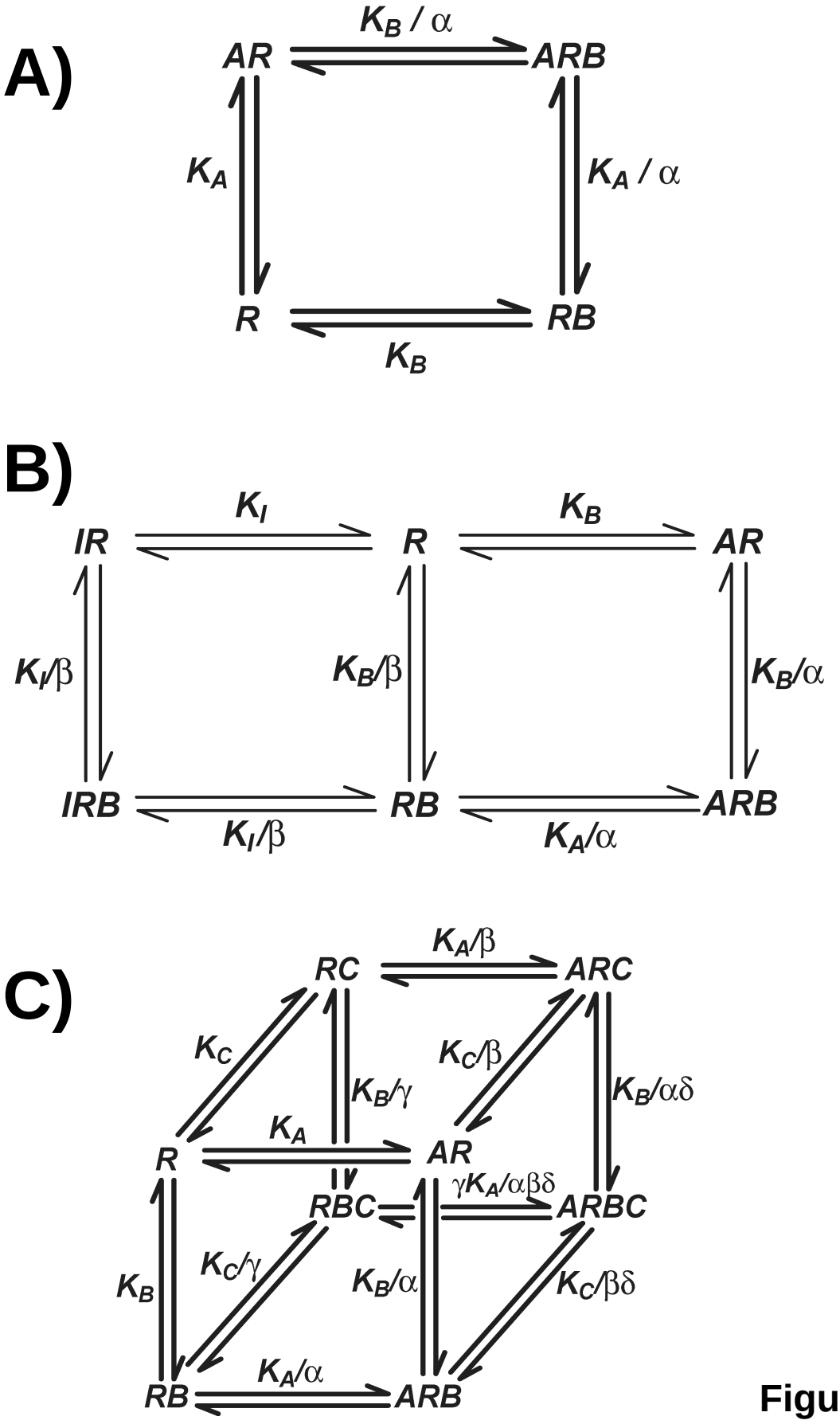

Figure 2

Molecular Pharmacology Fast Forward. Published on May 18, 2006 as DOI: 10.1124/mol.106.024711
This article has not been copyedited and formatted. The final version may differ from this version.

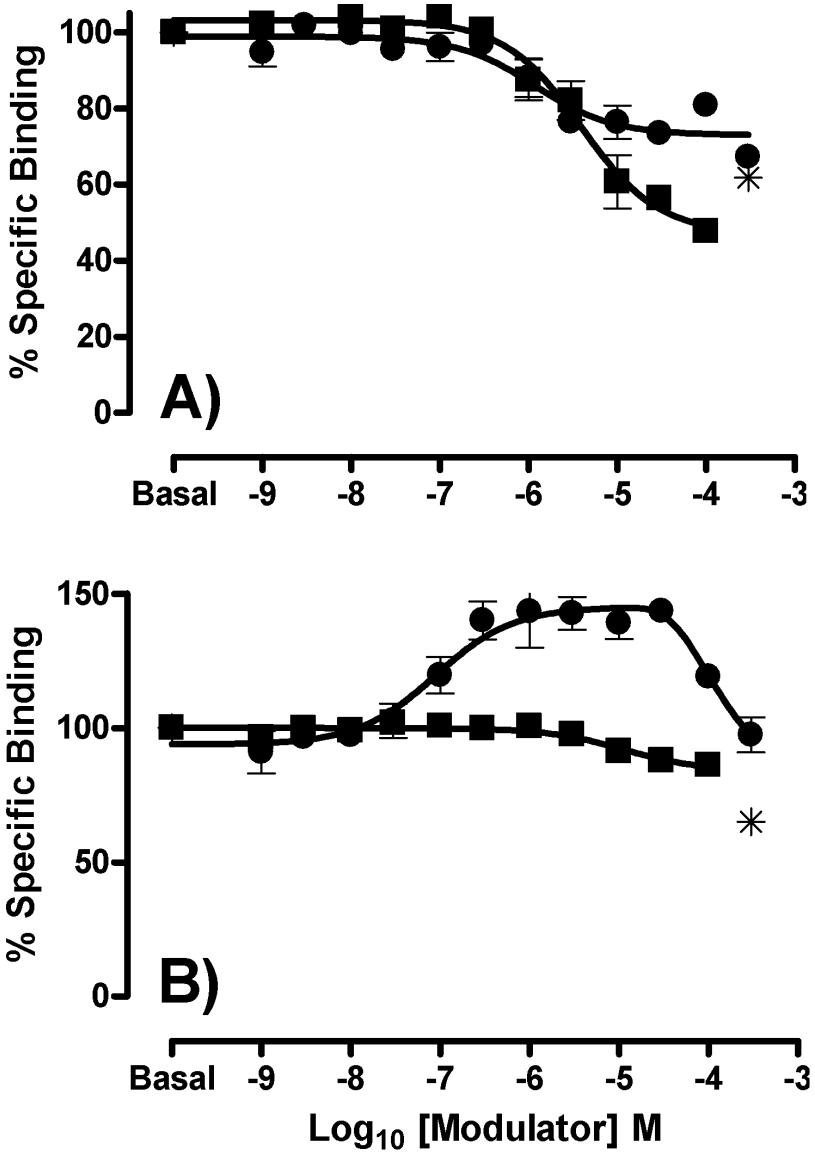

Figure 3

Molecular Pharmacology Fast Forward. Published on May 18, 2006 as DOI: 10.1124/mol.106.024711
This article has not been copyedited and formatted. The final version may differ from this version.

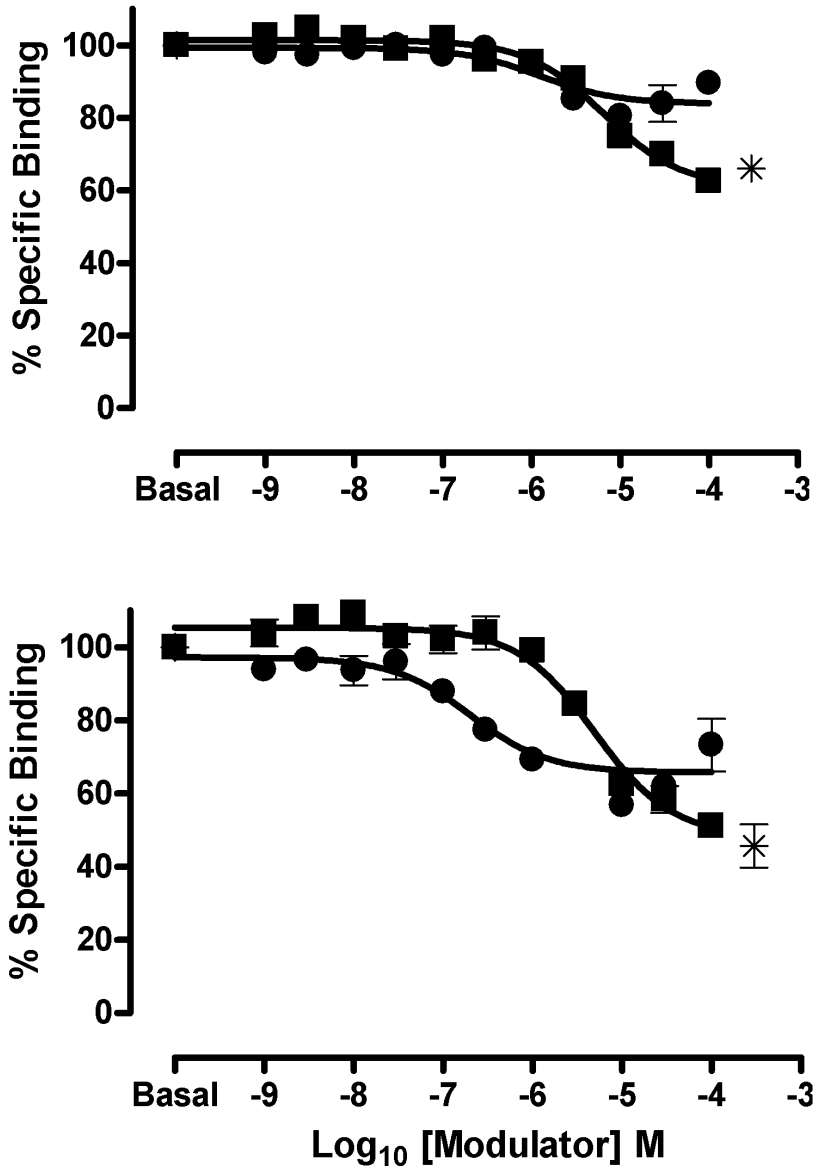

Figure 4

Molecular Pharmacology Fast Forward. Published on May 18, 2006 as DOI: 10.1124/mol.106.024711
This article has not been copyedited and formatted. The final version may differ from this version.

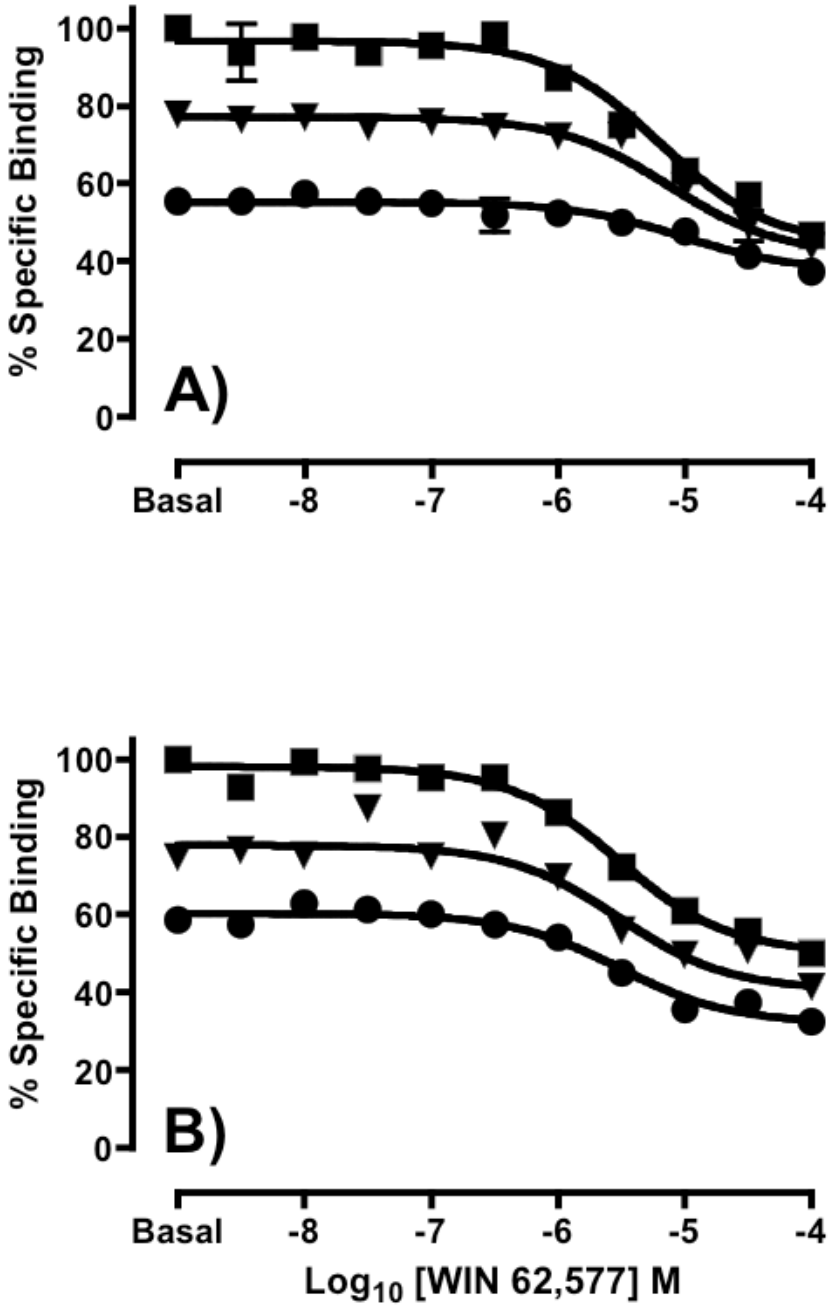

Figure 5

Molecular Pharmacology Fast Forward. Published on May 18, 2006 as DOI: 10.1124/mol.106.024711
This article has not been copyedited and formatted. The final version may differ from this version.

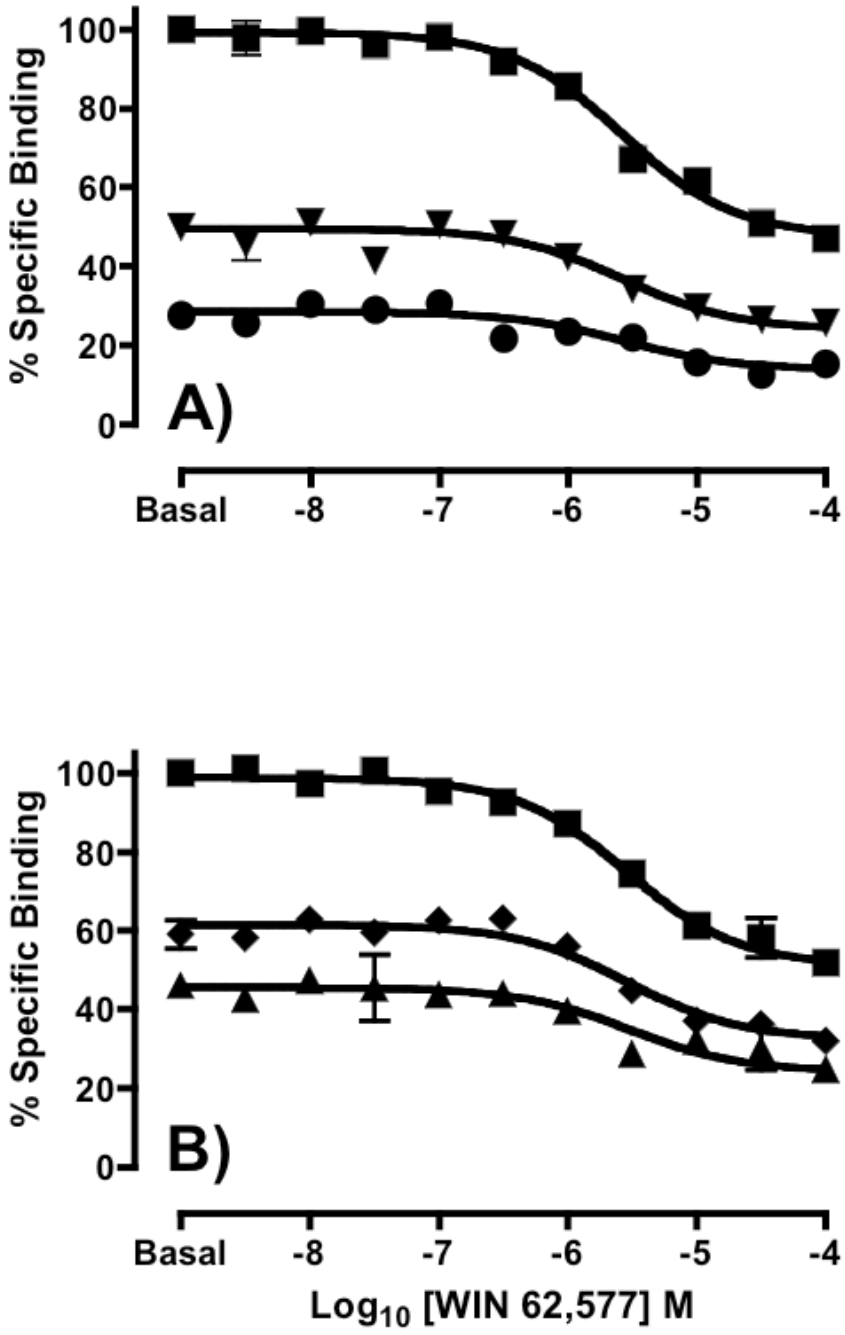

Figure 6

Molecular Pharmacology Fast Forward. Published on May 18, 2006 as DOI: 10.1124/mol.106.024711
This article has not been copyedited and formatted. The final version may differ from this version.

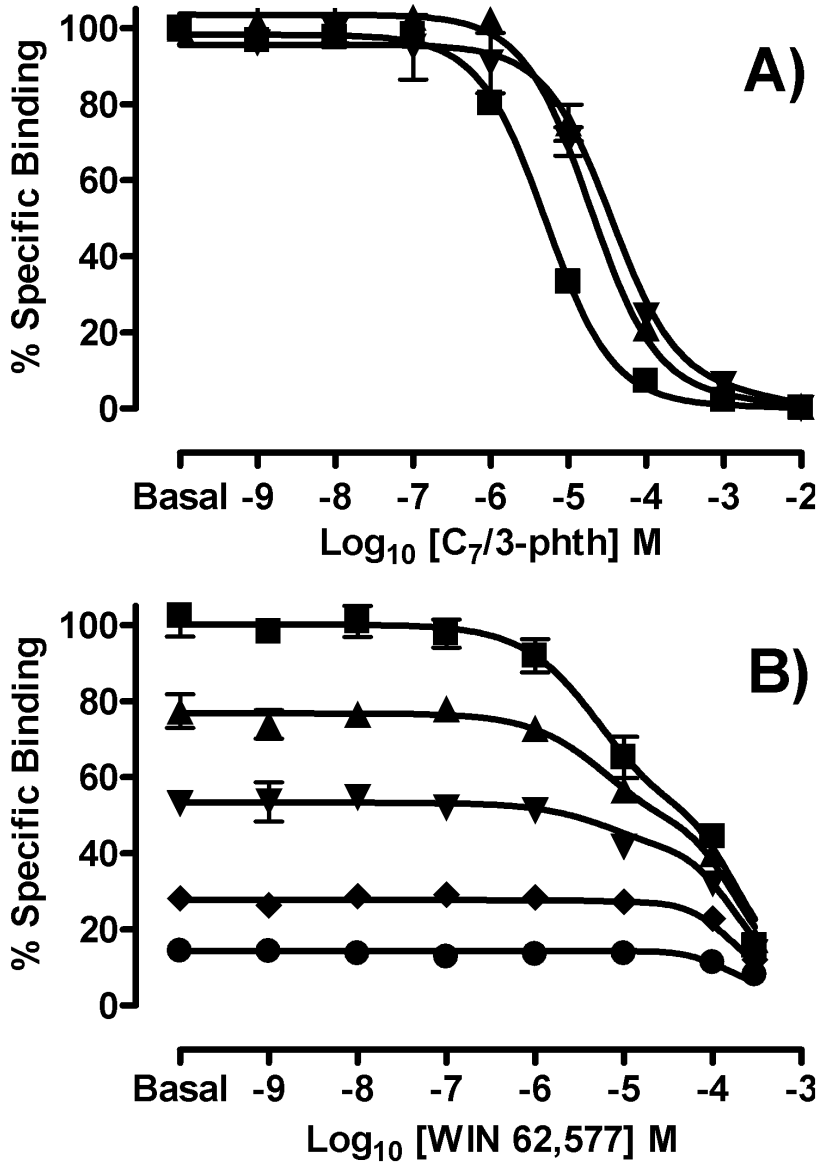

Figure 7

Molecular Pharmacology Fast Forward. Published on May 18, 2006 as DOI: 10.1124/mol.106.024711
This article has not been copyedited and formatted. The final version may differ from this version.

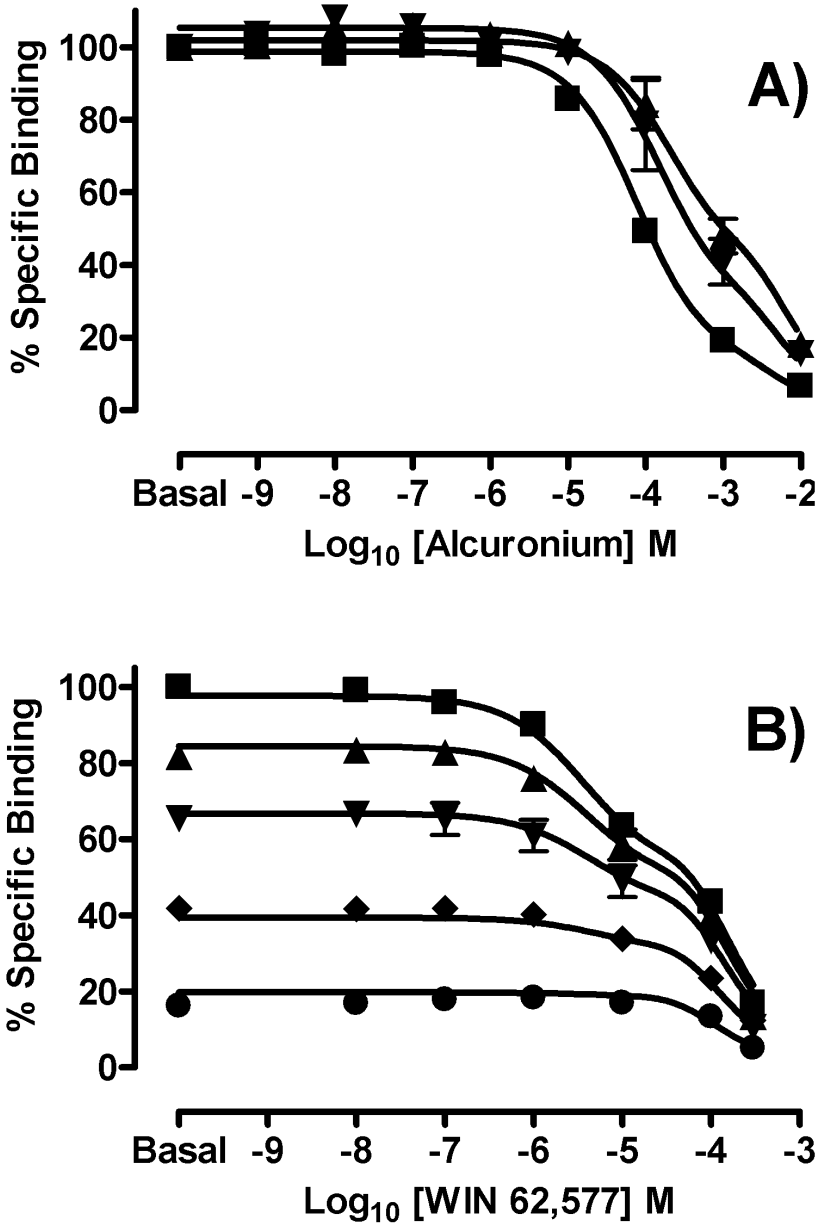

Figure 8

Molecular Pharmacology Fast Forward. Published on May 18, 2006 as DOI: 10.1124/mol.106.024711
This article has not been copyedited and formatted. The final version may differ from this version.

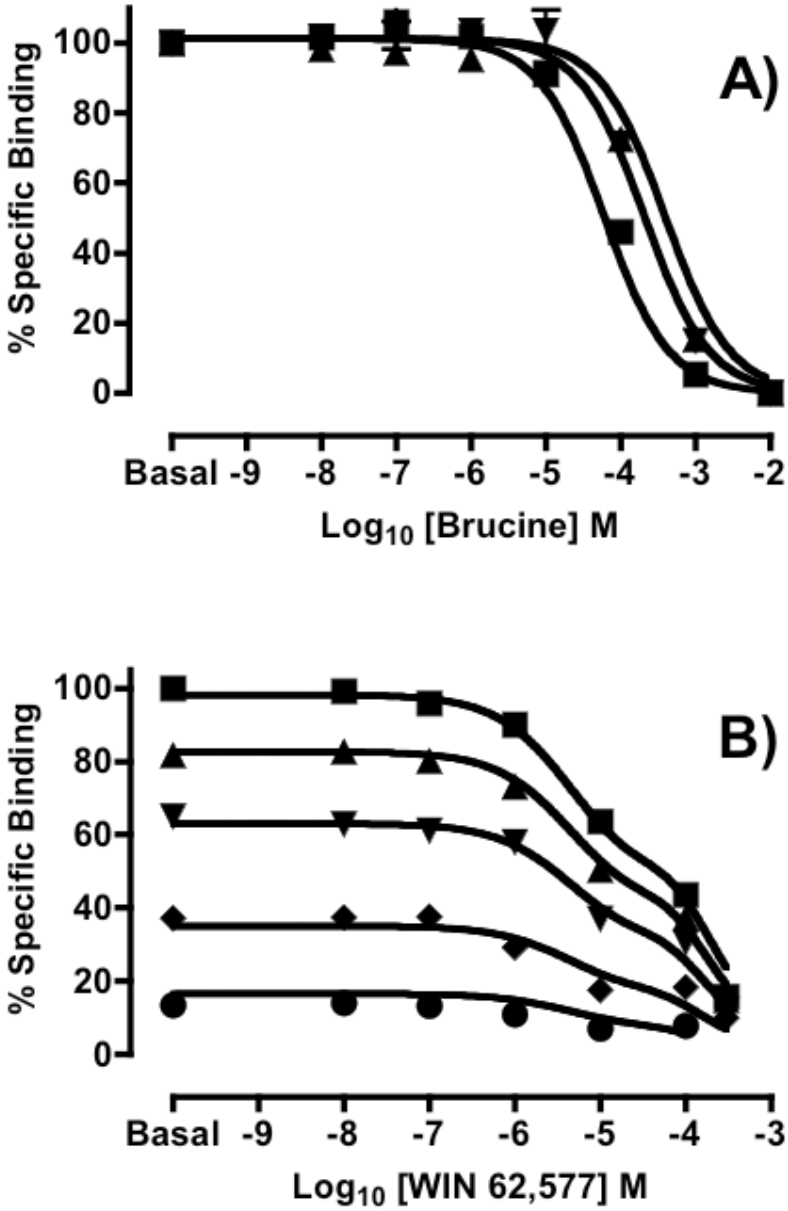

Figure 9

Molecular Pharmacology Fast Forward. Published on May 18, 2006 as DOI: 10.1124/mol.106.024711
This article has not been copyedited and formatted. The final version may differ from this version.

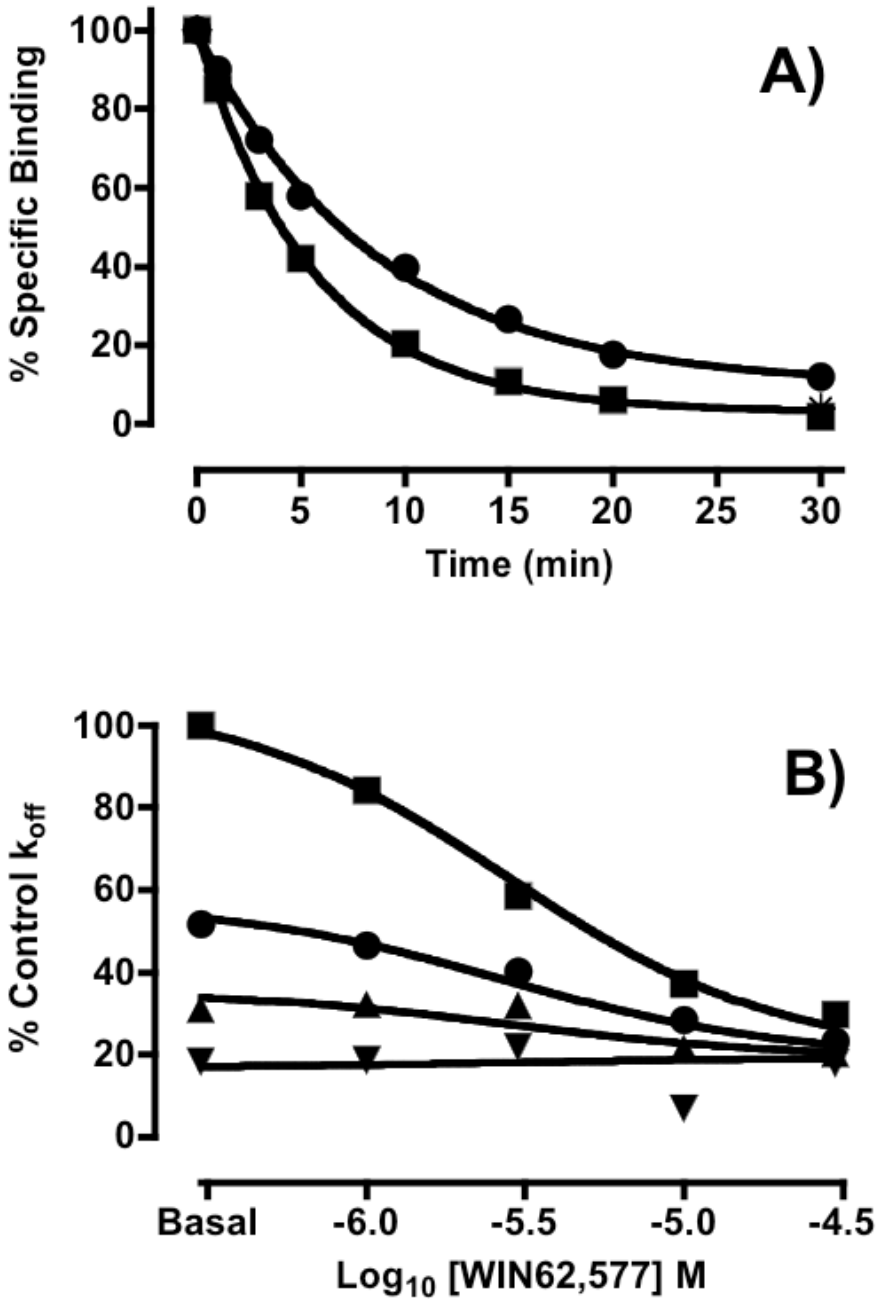

Figure 10